Steel and Composite Structures, *Vol. 29, No. 4 (2018) 557-567*
DOI: https://doi.org/10.12989/scs.2018.29.4.557

Buckling of axially compressed composite cylinders with geometric imperfections

Fathollah Taheri-Behrooz * and Milad Omidi [a]

School of Mechanical Engineering, Iran University of Science and Technology, Tehran, 16846-13114, Iran

(*Received October 12, 2017, Revised October 31, 2018, Accepted November 12, 2018*)

Abstract. Cylindrical shell structures buckle at service loads which are much lower than their associated theoretical buckling loads. The main source of this discrepancy is the presence of various imperfections which are created on the cylinder body during different processes as manufacturing, handling, assembling and machining. Many cylindrical shell structures are still designed against buckling based on the experimental data introduced by NASA SP-8007 as conservative lower bound curves. This study employed the numerical based Linear Buckling mode shape Imperfection (LBMI) method and modified it using a stochastic method to assess the effect of geometrical imperfections in more details on the buckling of cylindrical shells with and without the cutout. The comparison of results with those obtained from the numerical Simcple Perturbation Load Imperfection (SPLI) method for cylinders with and without cutout revealed a good correlation. The effect of two parameters of size and number of cutouts on the buckling load was investigated using the linear buckling and Modified LBMI methods. Results confirmed that in cylinders with a small cutout inserting geometrical imperfection using either SPLI or modified LBMI methods significantly reduced the value of the predicted buckling load. However, in cylinders with larger cutouts, the effect of the cutout is dominant, thus considering geometrical imperfection had a minor effect on the buckling loads predicted by both SPLI and modified LBMI methods. Furthermore, the modified LBMI method was employed to evaluate the combination effect of cutout numbers and size on the buckling load. It is shown that in small cutouts, an increasing in the cutout size up to a certain value resulted in a remarkable reduction of the buckling load, and beyond that limit, the buckling loads were constant against D/R ratios. In addition, the cutout number shows a more significant effect on decreasing the buckling load at small D/R ratios than large D/R ratios.

Keywords: buckling; composite; cylindrical shell; multiple cutout; geometric imperfections

1. Introduction

Fiber reinforced composites are widely used in aerospace structures due to their outstanding properties such as high strength and stiffness to weight ratios compared to traditional materials. In order to use the potential benefits of composite materials, new design methods need to be developed for strength and buckling of critical structures. For designing cylinders against buckling, some knock-down factors which rely on lower-bound curve are presented like as NASA SP-8007. But, this guideline is based on isotropic test results and for composite materials give conservative results that make structures heavier. So, new analysis procedures are under investigation by taking into account the properties of composite materials. So far, many analytical solutions have been developed to predict buckling load of the circular cylindrical shell with taking into account the effect of initial geometric imperfections such as Flugge (1932), Donnell (1934) and Koiter (1945). Ravenhall (1964) offered a correction factor to resolve the discrepancy between experiment and theory in circular cylindrical shells. For giving more information, Readers are referred to Tennyson (1975). Khayat *et al*. (2016) employed semi analytical Finite Strip Method (FSM) to investigate buckling and post buckling behavior of composite cylindrical shells. In 1960 NASA published a guideline curve Fig. 1 based on many tests which were performed and reported as NASA SP-8007. This guideline curve was introduced as a knock-down factor denoted by ρ in the term of radius to thickness ratio (R/t) for the isotropic cylindrical shell. It does not take into account the effect of boundary condition and ply sequence of orthotropic materials. The knock-down factor ρ for an isotropic materials was proposed by Seide *et al*. (1960) and then modified by Weingarten (1965) for orthotropic cylinders which is presented in Eq. (1).

$$\begin{gathered}\rho = 1 - 0.902(1 - e^{-\varphi}) \\ \varphi = \frac{1}{16}\sqrt{\frac{R}{t}} \qquad (Isotropic) \\ \varphi = \frac{1}{16}\sqrt{\frac{R}{t_{eq}}},\ t_{eq} = 3.46894\sqrt[4]{\frac{D_{11}D_{22}}{A_{11}A_{22}}} \quad (Orthotropic)\end{gathered} \tag{1}$$

Hutchinson and Koiter (1970) investigated the effect of imperfections on buckling of the circular cylindrical shell.

*Corresponding author, Professor,
E-mail: taheri@iust.ac.ir
[a] Graduate Student, E-mail: milad.omidi.mech@gmail.com

http://www.techno-press.org/?journal=scs&subpage=6
ISSN: 1229-9367 (Print), 1598-6233 (Online)

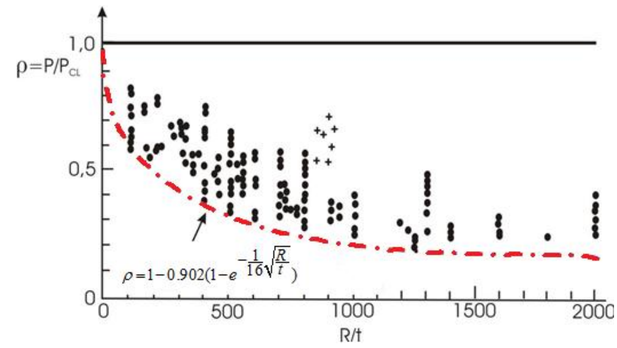

Fig. 1 NASA SP-8007 guideline curve

Khot (1968) employed the non-linear Donnell's theory and Card (Donnell 1969) used Koiter's theory along with the energy method to take into account the effect of imperfection on buckling load's capacity of composite cylindrical shells. They defined imperfection as an initial displacement in their procedures. The method of Linear Buckling Mode Imperfections (LBMI) was proposed by Khot and Venkayya (1970), they used the axially symmetric mode shapes obtained through linear eigenvalue buckling analysis as the initial imperfections in a cylindrical shell. However, selecting a suitable mode shape from linear analysis and appropriate coefficient magnitude are still under investigation.

Hilburger *et al*. (2006) examined geometric imperfections due to manufacturing signature and compared his results with LBMI method. Huhne *et al*. (2008) proposed a method to obtain buckling load by considering a local distortion in a local area of the shell structure. In their procedure, local perturbation was simulated by applying a lateral load and buckling was continued by applying the axial load. They found that after reaching to a certain lateral load, say P_1, cylinder lost sensitivity to lateral load, the corresponding axial load to P_1 was assigned the buckling load of the cylinder. This method is called Simple Perturbation Load Imperfections (SPLI) by Winterstetter and Schmidt (2002). Degenhardt *et al*. (2010) proposed a probabilistic stability analysis via Monte Carlo simulation and examined various imperfections such as geometrical, loading and material properties. They found that geometrical imperfections had the most important effect on axially buckling loads. In a comprehensive numerical investigation performed by Castro *et al.* (2014), several imperfections modeling methods are simulated numerically and results are compared and discussed. Shakouri *et al.* (2016) examined the effect of imperfection shapes on the buckling behavior of conical shells. Imperfection sensitivity to elastic buckling of wind loaded open cylindrical tanks was investigated by Godoy and Flores (2002). Buckling analysis of filament wound composite cylindrical shell for considering the filament undulation and crossover was examined by Guo *et al*. (2015). Effect of different length to radius ratio of cylinder (L/R) on knock-down factor was examined by Wagner *et al*. (2017). They proposed a numerical method of Single Boundary Perturbation Approach (SBPA) and compare their results with experiments and NASA SP-8007 guideline.

Hilburger *et al*. (1998, 1999) developed an analytical solution to predict buckling load of a composite cylinder with cutout. His predictions were in a good agreement with STAGS [1] (a finite element code for general-purpose nonlinear analysis of solid mechanic.) software and experimental data. Later Tafreshi (2002) showed Hilburger's results are well matched with ABAQUS software results. Orifici and Bisagni (2013) used the SPLI method to predict buckling load of composite cylinders with various size of square cutouts and stacking sequences. Arbelo *et al*. (2015) examined the effect of imperfections caused by SPLI method and cutout on composite cylindrical shells. They concluded that for small cutouts the effect of imperfections on buckling load is significant, whereas beyond a specified cutout size the knockdown effect due to imperfections is negligible compared to the effect of cutout itself. Moreover, in large cutouts combination of both effects are responsible for buckling load. Response of perforated glass/epoxy composite tubes subjected to axial compressive loading was investigated using numerical and experimental methods by Taheri-Behrooz *et al*. (2012).

This study have employed the numerical based Linear Buckling Mode shape Imperfection (LBMI) method to assess the effect of geometrical imperfections in more details on the buckling of cylindrical shells with and without cutouts. Furthermore, a stochastic linear mode shape selection criterian is coupled with well-known LBMI method to predict nonlinear buckling load of perforated and sound composite cylinders. Finally, the modified LBMI (M-LBMI) and the linear buckling analysis were employed to investigate a combination effect of cutout size and number on the cylindrical shell buckling behavior.

2. Finite element model preparation

The material used in this research is glass/epoxy, S2-449/SP 381, in the form of unidirectional tape with a thickness of one layer of 0.55 mm, stacking sequence of [90/23/-23/90] and a total wall thickness of 2.2 mm. The inner radius of the cylinder is 189 mm with 700 mm total length and 5 mm from both end of the cylinder is clamped, thus free length is 690 mm. Material properties of the composite layers are as: E_{11} = 47.1 GPa, E_{22} = 13.3 GPa, ϑ_{12} = 0.24, $G_{12} = G_{13} = G_{23}$ = 4.75 GPa according to Composite Materials Handbook (2002). Linear and non-linear solver of Abaqus-6.12 (Simulia 2012) were used to evaluate buckling behavior of the cylindrical shell numerically. Linear solver was used to calculate the buckling loads and their corresponding mode shapes. Non-linear solver in standard implicit with Newton-Raphson algorithm was used to obtain the load-end shortening response curves. The element type was standard shell with linear order and reduced integration, S4R. A mesh convergence analysis was performed with 92 elements in circumferential direction and 56 elements in axial direction so the mesh convergence study led to 5152 elements.

[1] Structural Analysis of General Shells

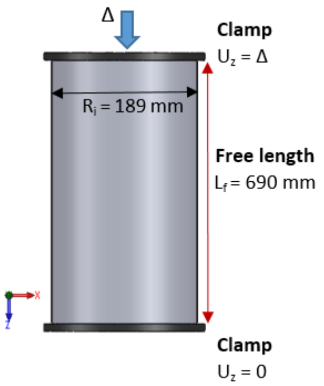

(a) Dimensions and boundary conditions

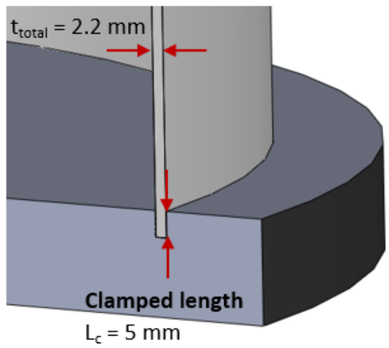

(b) Detailed view

Fig. 2 Dimensions and boundary conditions of the cylinder

Boundary conditions were clamped at both ends and loading condition was axial compression. Fig. 2(a) shows dimensions and boundary conditions in both ends of the cylinder and Fig. 2(b) shows a detailed view of the clamped end.

3. Buckling of the cylinder without cutout

There are several geometrical imperfections modeling methods which are used to predict buckling load of composite cylindrical shells (Castro *et al*. 2014). In this research Linear Buckling Mode shape Imperfections (LBMI) and Single Perturbation Load Imperfections (SPLI) are presented in details. A modified version of LBMI method is presented and compared with SPLI method predictions for the perfect composite cylinders.

3.1 Modified LBMI method for cylinders without cutout

Linear buckling analysis is a typical eigenvalue problem and gives mode shapes and buckling loads with linear analysis. These mode shapes which are appeared in the cylinder wall can be used as initial geometric imperfections. In LBMI method, mode shapes are tuned by applying a scaling factor and then are applied to the perfect cylinder as an initial imperfection to trigger buckling. To the best knowledge of the authors, it is not investigated which one of those mode shapes are dominant and more responsible for buckling of the cylinder under question. For composite cylinders, as shown in Table 1, different mode shapes have close buckling loads so that dominant mode shape cannot be selected solely due to the minimum buckling load of the structure. Moreover, it is not cleared what percentage of the selected mode shape would resulted in a realistic buckling load. Thus, there are two questions in the LBMI method which should be addressed, first: what eigenmode pattern is suitable? and second: what scaling factor of imperfections is acceptable? Table 1 illustrates the 30 first buckling mode shapes with associated buckling loads of the cylindrical shell. As, the buckling load of each even and its following odd mode shapes are almost the same so only the odd ones are presented in Table 1.

Fig. 3 shows buckling load with different eigenmode patterns as the initial imperfection at a constant scaling factor magnitude of $\delta/t = 0.2$. Moreover, buckling load with various scaling factor at first eigenmode pattern (selection of mode shape to study the effect of scaling factor is arbitrary) is shown. As shown in Table 1, linear buckling loads are close together for different mode shapes, for this reason predicted buckling loads by the LBMI method in a constant scaling factor shows small variation (Fig. 3). However, as shown in Fig. 3, the scaling factor at a constant modeshape (modeshape 1) had an important effect on the buckling load up to a certain limit of 0.6, beyond that limit the buckling load is constant. Worth to mention, by approaching the scaling factor to unity, applied mode shape as initial imperfection cease to be an imperfection and acts more like as a structural feature that changes the structure from a smooth cylinder to a corrugated cylinder which is out of the scope of this research.

Fig. 4 shows a variation of cylinder stiffness before buckling with different eigenmode patterns at a constant scaling factor of $\delta/t = 0.2$, and with various scaling factors at a constant mode shape. Increasing scaling factor resulted in remarkable reduction of cylinder's stiffness, while different mode shapes had a minor effect on it.

As is seen in Figs. 3 and 4, mode shapes used as imperfection pattern had a negligible effect on the predicted

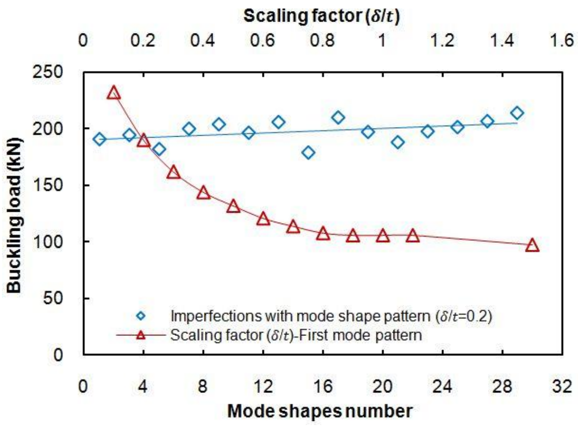

Fig. 3 Buckling load in different imperfections eigenmode patterns also different scaling factor (δ/t)

Table 1 Buckling mode shapes and associated loads

1st mode	3rd mode	5th mode	7th mode	9th mode	11th mode	13th mode	15th mode
			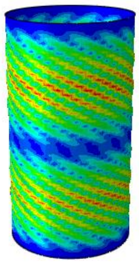	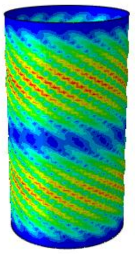	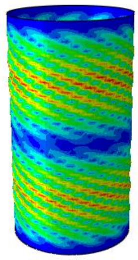	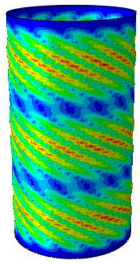	
325.55 kN	328.58 kN	329.32 kN	329.49 kN	332.14 kN	334.16 kN	335.98 kN	336.72 kN
17th mode	19th mode	21st mode	23rd mode	25th mode	27th mode	29th mode	
	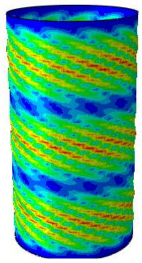	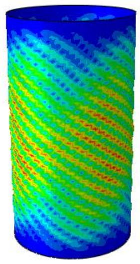	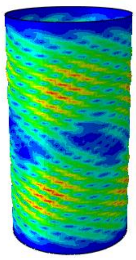			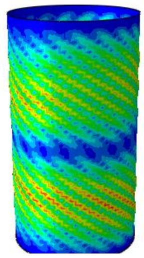	
338.02 kN	342.16 kN	342.33 kN	342.57 kN	344.94 kN	345.87 kN	346.22 kN	

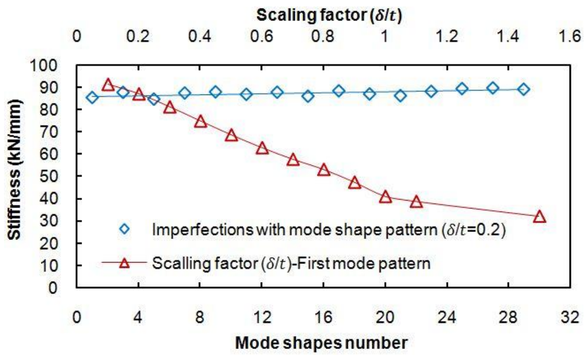

Fig. 4 Cylinder's stiffness in different imperfections and scaling factors (δ/t)

buckling load and the cylinder's stiffness using LBMI method. Thus in the present study, a stochastic approach was employed to select a possible happening eigenmode pattern among the thirty initial mode shapes. Fig. 5 shows the probability density functions for buckling load under different eigenmode patterns at a constant scaling factor (δ/t = 0.2). To obtain the probabilistic distribution as illustrated in Fig. 5, the thirty initial buckling mode shapes and their associated buckling loads were obtained using linear eigenvalue analysis. As the buckling loads of different mode shapes are close together, a probability distribution investigation was performed to select an eigenmode pattern which is more likely to occur during buckling analyses. Gaussian (normal) distribution is suitable for discrete numbers such as buckling loads. So its probability density function is calculated as follows

$$f\,(x) = \frac{1}{\sigma_x\sqrt{2\pi}}e^{\left(-\frac{1}{2}\left(\frac{x-\mu_x}{\sigma_x}\right)^2\right)} \tag{2}$$

Where, σ_x is the standard deviation, μ_x is the mean of data and 'x' is corresponded buckling load in each mode-shape.

By considering 30 initial mode shapes and calculation of their corresponding σ_x and μ_x, probability density function of each buckling load can be calculated. The mode shape associated with the buckling load with the maximum probability density function is the suitable eigenmode pattern which should be used in the M-LBMI method. As the buckling load of each even and its followed odd mode shapes are very close to each other, so only the odd ones are presented in Fig. 5. Circles on Fig. 5 are the representative of predicted buckling loads of each mode shape. According to Fig. 5, eigenmode 23rd has the maximum frequency, thus this mode shape is suitable for modeling imperfection pattern of the perfect composite cylinder.

In order to select the appropriate amplitude value for the candidate modeshape pattern as the initial imperfection,

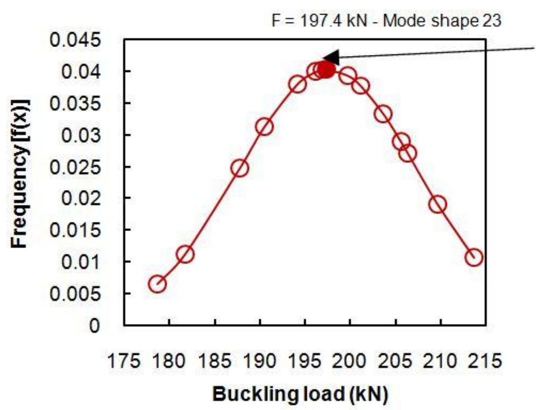

Fig. 5 Probabilistic distribution functions of buckling load in different eigenmode patterns

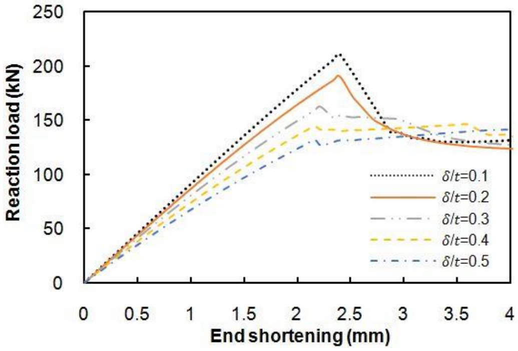

Fig. 6 Reaction load-End shortening curve in different scaling factors

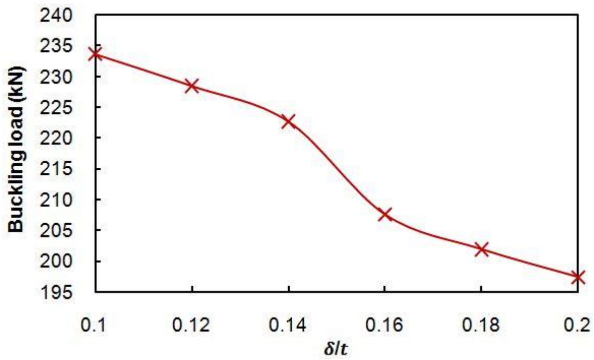

Fig. 7 Buckling load at 23rd eigenmode against imperfection amplitude ranged from 10 to 20 percent of thickness

experimental results obtained by Degenhardt *et al*. (2010) were used. Fig. 6 shows the reaction load versus end-shortening response curve in the 23^{rd} eigenmode pattern as initial imperfection under different scaling factors. As shown in Fig. 6, for scaling factors in the range of 10 to 20 percent of the wall thickness an abrupt change in the reaction load was observed while higher scaling factors resulted in smooth behavior after buckling.

Fig. 7 shows buckling load variations, at a constant imperfection given from 23^{rd} mode shape, against imperfection amplitude ranged from 10 to 20 percent of thickness. Due to safety issue considerations, the value of ‘‘small risk of failure” proposed by Franke (1987) was used and lower 0.5%-quantiles of the buckling load with scaling factor between 10 to 20 percent of thickness was taken as buckling load (201.98 kN).

3.2 SPLI method for cylinders without cutout

This type of imperfection was carried out by inserting a small amount concentrated load perpendicular to the cylinder axis prior to axial loading at the mid length of the cylinder. Buckling load is decreased by increasing SPL’s as demonstrated in Fig. 8. By approaching SPL’s to a certain value, the sensitivity of buckling load to SPL decreased and after that buckling load remain constant with increasing SPL. The corresponding load to this SPL is called P_1 and its associated axial load is buckling load, N_1.

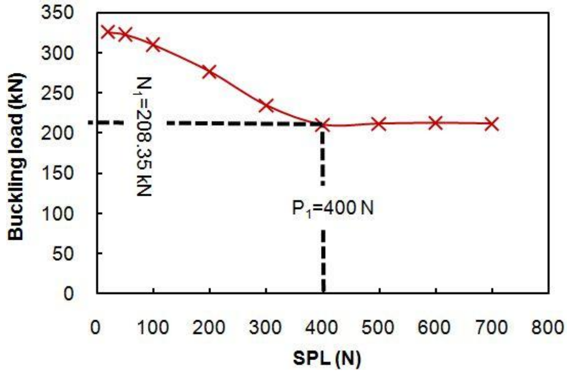

Fig. 8 Buckling load curve in different SPL

Fig. 9 shows reaction load against end-shortening curve in different SPL’s. As shown, in SPL’s ranged from 0 to 300N, the stiffness of structure up to buckling point was almost constant and abruptly changed in buckling moment. In SPL’s between 400 N to 500 N stiffness was constant until a local snap-through occurred in structure and caused deviation from initial stiffness, after that point reaction load was increased until global buckling happened. More than SPL about 600 N stiffness of structure would be decreased gradually until buckling occurred. The local snap-through pattern just before buckling, buckling pattern just after buckling and post-buckling pattern, are shown in Figs. 10(a)-(c), respectively.

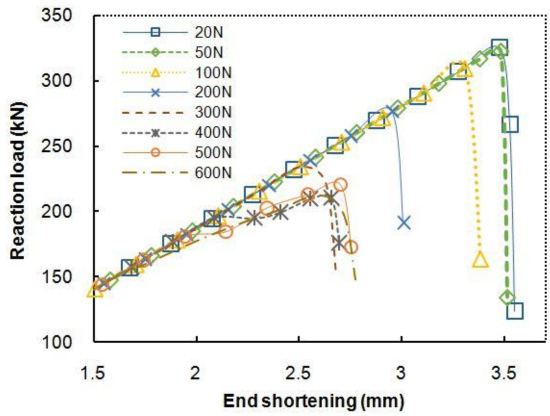

Fig. 9 Detailed reaction load in terms of end shortening in different SPL

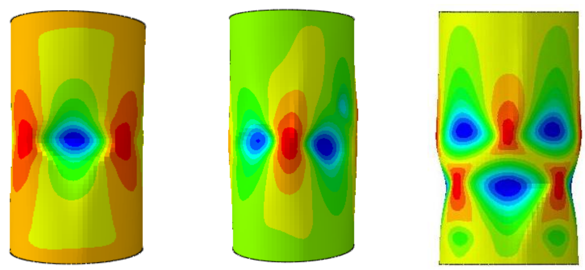

(a) Local snap-through (b) After buckling moment (c) Post-Buckling pattern

Fig. 10 Deformation in different states

3.3 Comparison between Modified LBMI and SPLI methods for cylinders without cutout

Fig. 11 comprises results obtained from two SPLI and M-LBMI methods which are presented in the current article. This is evidence that increasing amplitude of imperfections would decrease the buckling load predicted by two methods, however buckling load predicted by the LBMI method is always more conservative than those predicted by the SPLI method. This difference between results comes from different procedures which are used by two methods to define initial imperfections. Fig. 12(a) shows imperfections pattern in the overall structure of LBMI method and Fig. 12(b) shows perturbed position in SPLI method before buckling. In the LBMI method,

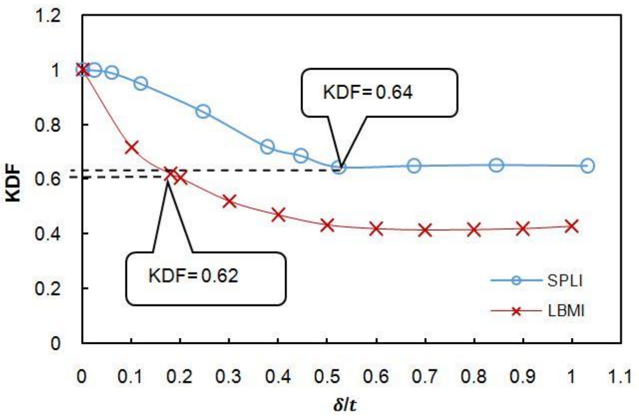

Fig. 11 Knock-down factor for the different amplitude of imperfections in SPLI and LBMI methods

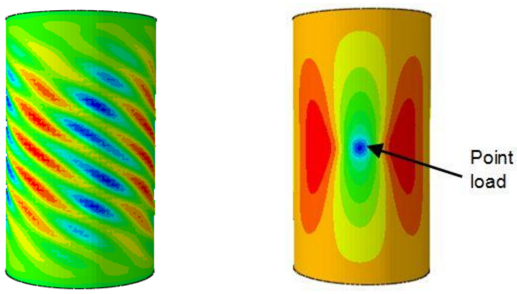

(a) LBMI method (b) SPLI method

Fig. 12 Imperfections pattern before buckling

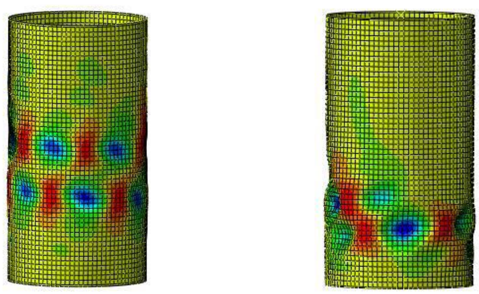

(a) LBMI method (b) SPLI method

Fig. 13 Buckling pattern just after buckling

Table 2 Predicted buckling load and associated knock-down factors

Method	Buckling load (kN)	KDF
Linear buckling analysis	325.55	1
NASA SP-8007	175.79	0.54
M-LBMI	201.98	0.62
SPLI	208.35	0.64

imperfections are applied all over the cylinder body while in the SPLI method imperfections are local and applied around the perturbation load. Thus imperfections engaged a major area of shell in LBMI in comparison to SPLI which would result in lower buckling load by the LBMI method. Predicted results by the SPLI and the Modified LBMI are close together. Figs. 13(a) and (b) show buckling pattern just after buckling in Modified LBMI and SPLI methods, respectively. Table 2 showed Knock-down factors and corresponding buckling loads predicted by Modified LBMI and SPLI methods also conservative results of NASA SP-8007.

4. Linear buckling of cylinders with cutout

When a cylindrical shell with a cutout is subjected to an axially compressive load, two phenomena are more likely to happen, buckling and static damage. Local buckling may occur in the body of shell structure without any sign of damage or damage may occur in the structure prior to the buckling phenomenon. In cylindrical shell with cutout, damage may occur prior to buckling in loading gripe area or around the cutouts region. In order to prevent premature damaging on the edge of loading or around cutouts, normally tabbing of the loading edges and stiffening of cutouts area are accomplished. Although dominant failure mode is depending on different parameters as cutout size and shell thickness, buckling of the cylinder is taken as the dominant failure mode in the current research.

In this article, cutouts are modeled with a circular shape and located in halfway along the axial length of the cylinder. Reinforcing around cutouts is neglected. Damage around cutout is not considered as a mode of failure prior to buckling. The effects of two geometrical parameters are investigated on buckling of a cylindrical shell with a cutout as size and number of cutouts. Fig. 14(a) shows circular cutouts with different sizes and Fig. 14(b) shows cylinder with a different number of cutouts. In this part, linear buckling is performed to evaluate the effect of these two parameters on buckling load of the cylinder. Worth to mention our research is limited to maximum four cutouts so presented results in the following subsections may not be valid for cylinders with multiple cutouts.

Local linear buckling behavior of the cylinder with a circular cutout is shown in Fig. 15. As illustrated in Fig. 15 number of cutouts has minor effect on the buckling load of the cylinder while the size of the cutouts revealed remarkable effects. The sensitivity of the buckling load to the cutout size was decreased beyond a certain cutout size.

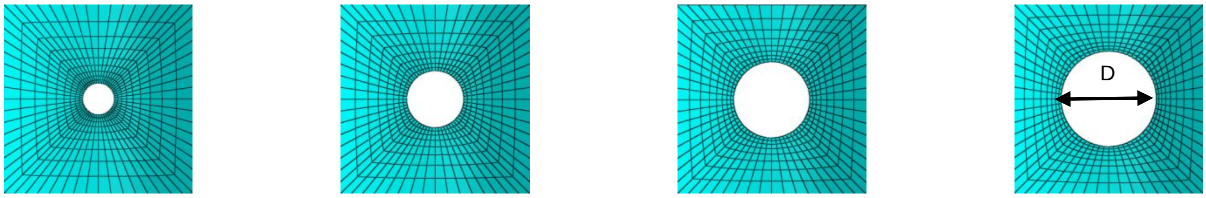

D = 40 mm D = 60 mm D = 80 mm D = 100 mm

(a) Size of cutout

Single cutout Two-cutout Three-cutout Four-cutout

(b) Number of cutout

Fig. 14 Geometrical parameters of cylinders with cutout

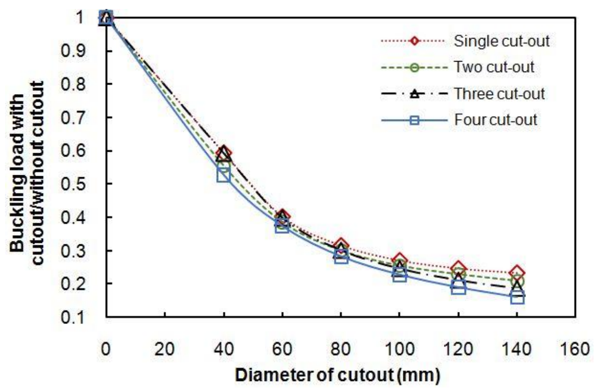

Fig. 15 Buckling load with different size and number of cutouts

In the following section, Modified LBMI method is used to evaluate the effect of size and number of the cutout on the buckling load of a cylindrical shell structure. Worth to mention, as the non-linear buckling of a cylinder with square cutout was investigated previously by Orifici and Bisagni (2013), therefore this research is focused solely on the cylinder with a circular cutout.

4.1 Modified LBMI method for cylinder with cutout

Eigenmodes extracted by linear buckling analysis for a cylindrical shell containing a single circular cutout of 50mm diameter are exhibited in Table 3. In contrast to buckling load of a perfect cylinder, every mode shape of a cylinder with cutout has its corresponding buckling load. Mode

Table 3 Buckling mode shapes in a cylinder with circular cutout and associated buckling load

1st mode	2nd mode	3rd mode	4th mode	5th mode	6th mode	7th mode	8th mode
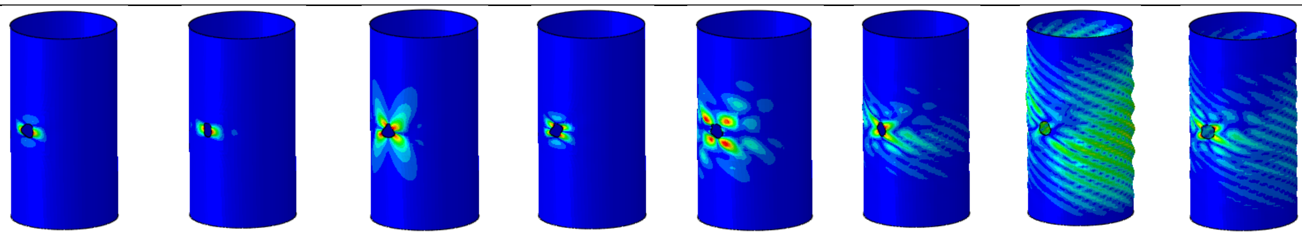							
157.64 kN	161.12 kN	166.42 kN	216.06 kN	309.27 kN	321.39 kN	325.09 kN	325.57 kN
9th mode	10th mode	11th mode	12th mode	13th mode	14th mode	15th mode	
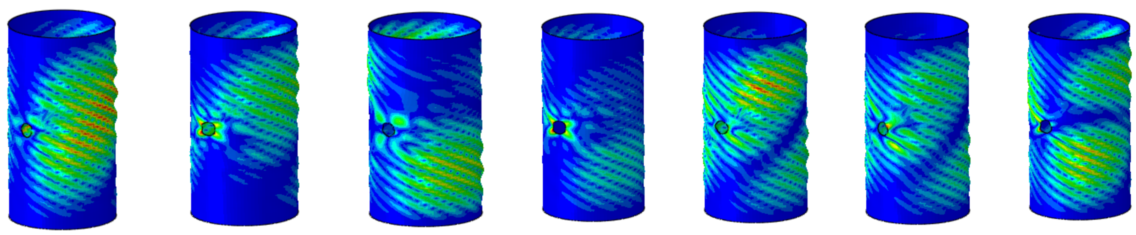							
328.48 kN	328.95 kN	329.12 kN	329.34 kN	330.8 kN	330.92 kN	332.31 kN	

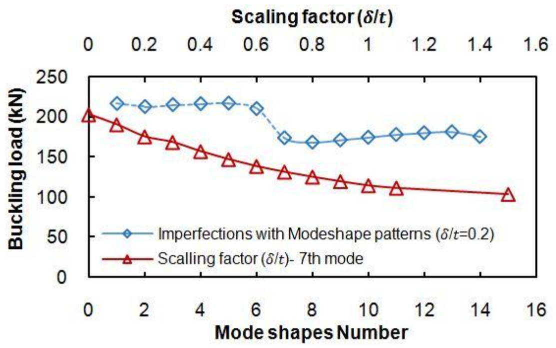

Fig. 16 Buckling load against different eigenmode patterns and scaling factors for a cylinder with a 50 mm cutout

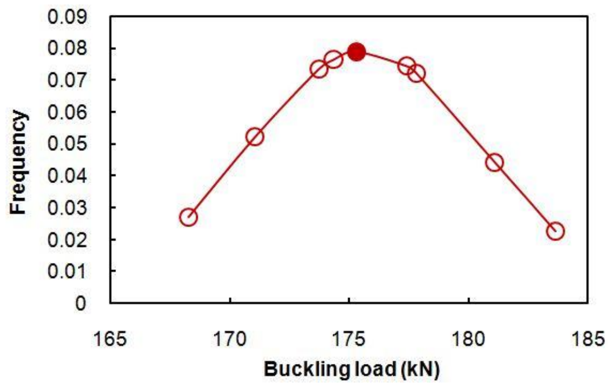

Fig. 18 The probabilistic distribution function of buckling load for a cylinder with 50 mm cutout

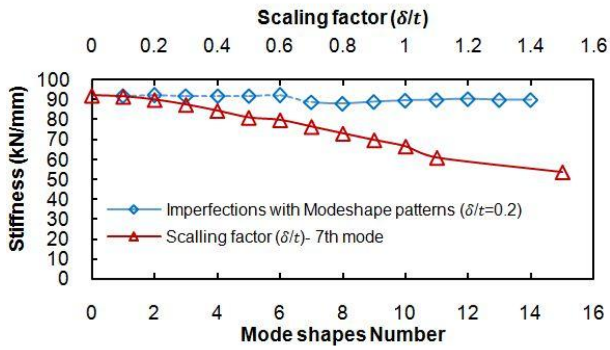

Fig. 17 Stiffness against different eigenmode patterns and scaling factors for a cylinder with 50 mm cutout

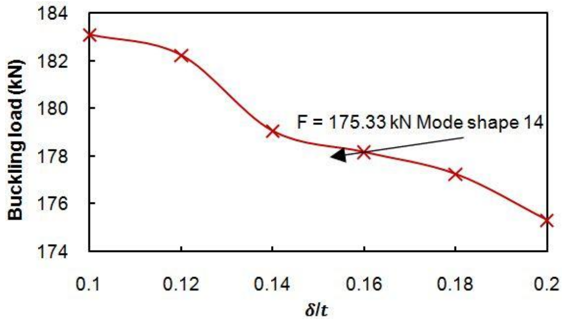

Fig. 19 Buckling load with imperfection amplitude between 10 to 20 percent of thickness and eigenmode pattern of 14

shapes can be classified in two folds, a series of mode shapes just consist of deformation around cutouts that predict local buckling while the other mode shapes are related to global buckling of the cylinder. As shown in Table 3 first six modes are associated with local buckling and the rest are for global buckling. Fig. 16 shows buckling load with different imperfections eigenmode pattern at constant imperfection magnitude of δ/t = 0.2, furthermore buckling load with various scaling factors at a constant imperfection eigenmode pattern of 7th mode (selection of mode shape to study the effect of scaling factor was arbitrary). It is worth pointing out, as local buckling modes (1 to 6) are related to deformations around the cutouts not whole of the cylinder so global mode shapes are considered as initial imperfections in the M-LBMI method which is introduced in the current research. As shown in Fig. 16, imperfection patterns selected from mode 1 to 6 that marked with dashed line give buckling loads close together while the remaining modes result in buckling loads remarkably lower than first six eigenmodes. By increasing magnitude of imperfections, buckling load was decreased constantly without converging to a constant value. Fig. 17 shows stiffness of structure with different imperfections eigenmode pattern at a constant imperfection magnitude of δ/t = 0.2, furthermore stiffness of structure with imperfections eigenmode pattern given from 7th mode against different scaling factor for 50mm cutout. Similar to cylinder without cutout, different imperfections due to eigenmode patterns resulted in almost same stiffness before buckling. Even though stiffness in cylinder with imperfection due to local eigenmode patterns (modes 1 to 6) are somewhat higher than imperfections due to global eigenmode patterns. As shown in Figs. 16 and 17 scaling factor has more important effect on buckling behavior of perforated cylinder than eigenmode pattern.

As discussed in previous section, a stochastic procedure is used to select the suitable mode shape pattern as the initial imperfection for non-linear analysis of the perforated cylinder. In Fig. 18 probabilistic density function is drawn for different buckling load from global eigenmode patterns (modes 7 to 15). The maximum frequency in predicting buckling load is related to mode shape number 14th, which will be used as imperfection pattern to predict the buckling load of the cylinder with a cutout in Modified LBMI method.

Fig. 19 shows the buckling load with imperfections amplitude ranged from 10 to 20 percent of thickness at 14th mode shape. For lowest risk in buckling load prediction, lower 0.5%-quantiles of buckling load with scaling factor between 10 to 20 percent of thickness was taken as buckling load (175.33 kN).

Modified LBMI method was employed to evaluate the combination effect of cutout numbers and size on the buckling load. It was shown in Fig. 20 that in small cutouts, increasing cutout size up to a certain value resulted in a remarkable reduction of the buckling load, beyond that limit buckling load were constant against D/R ratios. Moreover, the cutout number had a major effect on decreasing of the buckling load at small D/R ratios than large D/R ratios

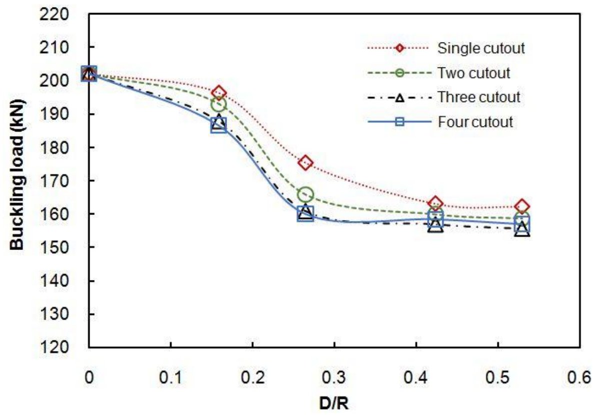

Fig. 20 Buckling load against different D/R ratios for 1-4 cutouts

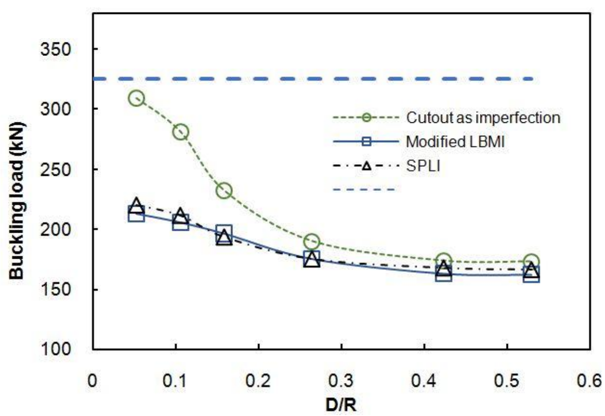

Fig. 23 Buckling load against D/R ratios of the cylinder

based on our observation for 1 to 4 cutouts and the specific cylinder under question.

4.2 SPLI method for cylinder with cutout

Orifisi and Bisagni (2013) examined buckling of composite cylindrical shells with square shape cutouts by using the SPLI method. In this article cutouts with circular shape are investigated by SPLI method and results are compared with Modified LBMI method. In order to evaluate the effect of horizontal perturbation load location on the buckling load, two points as “A” far away from cutout and “B” on the edge of cutout was selected as shown in Fig. 21.

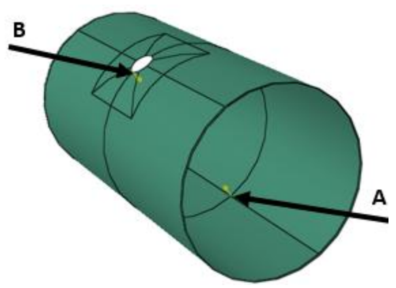

Fig. 21 Local of applying perturbation load, “A” far away from the cutout, “B” on the edge of the cutout

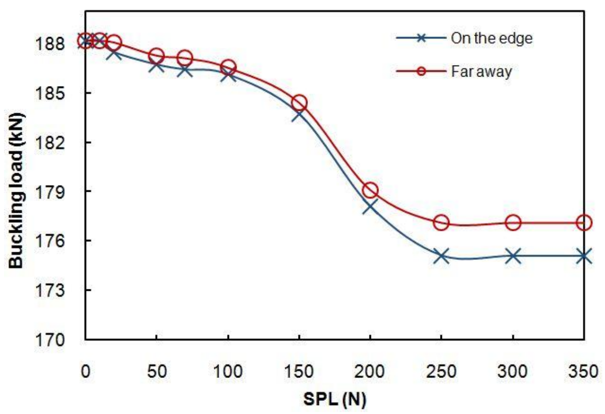

Fig. 22 Buckling load in SPLI method for a cylinder with cutout diameter of 50 mm

Fig. 22 illustrated buckling load predicted by SPLI method for the different position of initial perturbation as on the edge of the cutout and far from it. Buckling load with perturbation load on the edge of cutout converged to 175.11 kN while for perturbation load far away from cutout converged to 177.12 kN. Both results are near to predicted buckling load by a nonlinear method without considering perturbation. However, since instability initiation is around the cutout so perturbation on the edge of the hole gives lower buckling load than perturbation far away from the hole. The predicted buckling load with perturbation on the edge of the cutout (175.11 kN) could be a conservative selection.

4.3 Combination effect of cutouts and geometric imperfections on the buckling load

Buckling loads are predicted for a cylinder with various cutout diameters using different methods. As cutout on the cylinder act as an imperfection, so its effect was investigated separately using nonlinear methods and results are compared with predicted results using both LBMI and SPLI methods. Fig. 23 shows the buckling load against different cutout diameter to the radius of cylinder ratio (D/R) using different methods. Circular symbols in Fig. 23 illustrate the effect of the cutout on the buckling load without considering any other geometrical imperfections. Square and triangle symbols, in Fig. 23, are corresponding to the buckling loads predicted by the Modified LBMI and SPLI methods, respectively. As depicted in Fig. 23 for small cutouts the effect of the cutout and geometrical imperfections are important and should be considered in buckling load calculations, while for the larger cutouts geometrical imperfections have an ignorable effect and nonlinear solution gives acceptable results.

5. Conclusions

An investigation on the buckling of composite cylindrical shells with and without cutout was performed with using linear buckling mode shape imperfection (LBMI) and simple perturbation load imperfection (SPLI) approaches. A modification was suggested to enhance the ability of LBMI method to predict the critical buckling load of thin-walled cylindrical shell structures. As the linear buckling loads of composite cylindrical shells were very close to each other, so a stochastic approach was developed to select the eigenmode pattern with the maximum frequency in the probability density function chart. The predicted results with using the modified LBMI method were compared with results of SPLI method to assess the ability of M-LBMI method. The results of the SPLI and Modified LBMI methods in cylindrical shells without cutout were close together but higher than the buckling load predicted by the linear buckling analysis modified by NASA SP-8007 knockdown factors. In the second part of the current manuscript, buckling loads of the perforated cylindrical shells was investigated by considering the effects of imperfection pattern, size and number of cutouts on the cylinder's body. The results obtained by both of the SPLI and Modified LBMI methods revealed that considering geometrical imperfection in the buckling analysis resulted in a significant decrease in the value of the predicted buckling load in cylindrical shells with small cutouts. However, in cylinders with larger cutouts, the effect of the cutout is dominant. So considering geometrical imperfection had a minor effect on the buckling load predicted by both of the SPLI and modified LBMI methods. Moreover, Modified LBMI method was employed to evaluate the combination effect of cutout numbers and size on the buckling load. It was shown that in small cutouts, increasing cutout size up to a certain value resulted in a remarkable reduction of the buckling load, beyond that limit the buckling loads were constant against D/R ratios. Moreover, cutout number had more effect on decreasing of the buckling load at small D/R ratios than large D/R ratios.

References

Arbelo, M.A., Herrmann, A., Castro, S.G., Khakimova, R., Zimmermann, R. and Degenhardt, R. (2015), "Investigation of buckling behavior of composite shell structures with cutouts", *Appl. Compos. Mater.*, **22**(6), 623-636.

Card, M.F. (1969), "The sensitivity of buckling of axially compressed fiber-reinforced cylindrical shells to small geometric imperfections", NASA TMX-61914.

Castro, S.G., Zimmermann, R., Arbelo, M.A., Khakimova, R., Hilburger, M.W. and Degenhardt, R. (2014), "Geometric imperfections and lower-bound methods used to calculate knock-down factors for axially compressed composite cylindrical shells", *Thin-Wall. Struct.*, **74**, 118-132.

Composite Materials Handbook, MIL-HDBK-17-2F (2002), *Polymer Matrix Composites Materials Properties*, Volume 2.

Degenhardt, R., Kling, A., Bethge, A., Orf, J., Kärger, L., Zimmermann, R. and Calvi, A. (2010), "Investigations on imperfection sensitivity and deduction of improved knock-down factors for unstiffened CFRP cylindrical shells", *Compos. Struct.*, **92**(8), 1939-1946.

Donnell, L.H. (1934), "A new theory for the buckling of thin cylinders under axial compression and bending", *Trans. Asme*, **56**(11), 795-806.

Flügge, W. (1932), "Die stabilität der Kreiszylinderschale", *Ingenieur-Archiv*, **3**(5), 463-506.

Franke, W.D. (1987), "FMEA Fehlermglichkeits- und -einflußanalyse in der industriellen Praxis", *Moderne Industrie*, Landsberg, Germany.

Godoy, L.A. and Flores, F.G. (2002), "Imperfection sensitivity to elastic buckling of wind loaded open cylindrical tanks", *Struct. Eng. Mech., Int. J.*, **13**(5), 533-542.

Guo, Z., Han, X., Guo, M. and Han, Z. (2015), "Buckling analysis of filament wound composite cylindrical shell for considering the filament undulation and crossover", *Struct. Eng. Mech., Int. J.*, **55**(2), 399-411.

Hilburger, M.W., Waas, A.M. and Starnes, Jr., J.H. (1998), "A numerical and experimental study of the response of selected compression-loaded composite shells with cutouts", *Proceedings of the 39th AIAA/ASME/ASCE/AHS/ASC Structures, Structural Dynamics and Materials Conference*, Long Beach, CA, USA, AIAA 98-1768.

Hilburger, M.W., Waas, A.M. and Starnes, J.H. (1999), "Response of composite shells with cutouts to internal pressure and compression loads", *AIAA Journal*, **37**(2), 232-237.

Hilburger, M.W., Nemeth, M.P. and Starnes, J.H. (2006), "Shell buckling design criteria based on manufacturing imperfection signatures", *AIAA Journal*, **44**(3), 654-663.

Hühne, C., Rolfes, R., Breitbach, E. and Teßmer, J. (2008), "Robust design of composite cylindrical shells under axial compression—simulation and validation", *Thin-Wall. Struct.*, **46**(7), 947-962.

Hutchinson, J.W. and Koiter, W.T. (1970), "Postbuckling theory", *Appl. Mech. Rev.*, **23**(12), 1353-1366.

Khayat, M., Poorveis, D. and Moradi, S. (2016), "Buckling analysis of laminated composite cylindrical shell subjected to lateral displacement-dependent pressure using semi-analytical finite strip method", *Steel Compos. Struct., Int. J.*, **22**(2), 301-321.

Khot, N.S. (1968), "On the influence of initial geometric imperfections on the buckling and postbuckling behavior of fiber-reinforced cylindrical shells under uniform axial compression (No. AFFDL-TR-68-136)", Air force flight dynamics lab wright-oatterson AFB OH.

Khot, N.S. and Venkayya, V.B. (1970), "Effect of fiber orientation on initial postbuckling behavior and imperfection sensitivity of composite cylindrical shells (No. AFFDL-TR-70-125)", Air force flight dynamics lab wright-oatterson AFB OH.

Koiter, W.T. (1945), *A Translation of the Stability of Elastic Equilibrium*, Tech. Hooge School.

Orifici, A. and Bisagni, C. (2013), "Perturbation-based imperfection analysis for composite cylindrical shells buckling in compression", *Compos. Struct.*, **106**, 520-528.

Ravenhall, R. (1964), "Stiffness and buckling in filament-wound motors", *J. Spacecr. Rockets*, **1**(3), 260-263.

Seide, P., Weingarten, V.I. and Morgan, E.J. (1960), "The development of design criteria for elastic stability of thin shell structures (No. EM-10-26)", TRW Space Technology Labs Los Angeles, CA, USA.

Shakouri, M., Spagnoli, A. and Kouchakzadeh, M.A. (2016), "Effects of imperfection shapes on buckling of conical shells under compression", *Struct. Eng. Mech., Int. J.*, **60**(3), 365-386.

Simulia, D.S. (2012), Abaqus 6.12 Analysis User's Manual, Providence, RI, USA.

Tafreshi, A. (2002), "Buckling and post-buckling analysis of composite cylindrical shells with cutouts subjected to internal pressure and axial compression loads", *Int. J. Press. Vessels Pip.*, **79**(5), 351-359.

Taheri-Behrooz, F., Esmaeel, R.A. and Taheri, F. (2012), "Response of perforated glass/epoxy composite tubes subjected to axial compressive loading", *Thin-Wall. Struct.*, **50**, 174-181.

Tennyson, R.C. (1975), "Buckling of laminated composite cylinders: a review", *Composites*, **6**(1), 17-24.

Wagner, H.N.R., Hühne, C., Niemann, S. and Khakimova, R. (2017), "Robust design criterion for axially loaded cylindrical

shells-Simulation and Validation", *Thin-Wall. Struct.*, **115**, 154-162.
Weingarten, V.I. and Seide, P. (1965), "Elastic stability of thin-walled cylindrical and conical shells under combined external pressure and axial compression", *AIAA J.*, **3**(5), 913-920.
Winterstetter, T.A. and Schmidt, H. (2002), "Stability of circular cylindrical steel shells under combined loading", *Thin-Wall. Struct.*, **40**(10), 893-910.

CC